Research Repository UCD

Title	Paracrine signalling of inflammatory cytokines from an in vitro blood brain barrier model upon exposure to polymeric nanoparticles
Authors(s)	Nic Raghnaill, Michelle, Bramini, Mattia, Ye, Dong, Åberg, Christoffer, Salvati, Anna, Lynch, Iseult, Dawson, Kenneth A., et al.
Publication date	2014-03
Publication information	Nic Raghnaill, Michelle, Mattia Bramini, Dong Ye, Christoffer Åberg, Anna Salvati, Iseult Lynch, Kenneth A. Dawson, and et al. "Paracrine Signalling of Inflammatory Cytokines from an in Vitro Blood Brain Barrier Model upon Exposure to Polymeric Nanoparticles." Royal Society of Chemistry, March 2014. https://doi.org/10.1039/C3AN01621H.
Publisher	Royal Society of Chemistry
Item record/more information	http://hdl.handle.net/10197/5194
Publisher's version (DOI)	10.1039/C3AN01621H

Downloaded 2026-05-01 23:36:35

The UCD community has made this article openly available. Please share how this access benefits you. Your story matters! (@ucd_oa)

© Some rights reserved. For more information

Paracrine signalling of inflammatory cytokines from an in vitro blood brain barrier model upon exposure to polymeric nanoparticles

Michelle Nic Raghnaill,[a] Mattia Bramini,[a] Dong Ye,[a] Pierre-Olivier Couraud,[b] Ignacio A. Romero,[c] Babette Weksler,[d] Christoffer Åberg,[a] Anna Salvati,[a] Iseult Lynch,[a,‡] Kenneth A. Dawson*[a]

[a] Centre for BioNano Interactions, School of Chemistry and Chemical Biology, University College Dublin, Belfield, Dublin 4, Ireland. E-mail: kenneth.a.dawson@cbni.ucd.ie

[b] Institute COCHIN, CNRS (UMR 8104), INSERM U567, University of Paris Descartes, Paris, France

[c] Department of Biological Sciences, Open University, Walton Hall, Milton Keynes, United Kingdom

[d] Weill Cornell Medical College, New York, NY 10065, United States

[‡] Current address: School of Geography, Earth and Environmental Sciences, University Of Birmingham, Edgbaston, Birmingham B15 2TT, United Kingdom

Abstract

Nanoparticle properties, such as small size relative to large highly modifiable surface area, offer great promise for neuro-therapeutics and nanodiagnostics. A fundamental understanding and control of how nanoparticles interact with the blood-brain barrier (BBB) could enable major developments in nanomedical treatment of previously intractable neurological disorders, and help ensure that nanoparticles not intended to reach the brain do not cause adverse effects. Nanosafety is of utmost importance to this field. However, a distinct lack of knowledge exists regarding nanoparticle accumulation within the BBB and the biological effects this may induce on neighbouring cells of the Central Nervous System (CNS), particularly in the long-term. This study focussed on the exposure of an *in vitro* BBB model to model carboxylated polystyrene nanoparticles (PS COOH NPs), as these nanoparticles are well characterised for *in vitro* experimentation and have been reported as non-toxic in many biological settings. TEM imaging showed accumulation but not degradation of 100 nm PS COOH NPs within the lysosomes of the *in vitro* BBB over time. Cytokine secretion analysis from the *in vitro* BBB post 24 h 100 nm PS COOH NP exposure showed a low level of pro-inflammatory RANTES protein secretion compared to control. In contrast, 24 h exposure of the *in vitro* BBB endothelium to 100 nm PS COOH NPs in the presence of underlying astrocytes caused a significant increase in pro-survival signalling. In conclusion, the tantalising possibilities of nanomedicine must be balanced by cautious studies into the possible long-term toxicity caused by accumulation of known 'toxic' and 'non-toxic' nanoparticles, as general toxicity assays may be disguising significant signalling regulation during long-term accumulation.

Introduction

The brain endothelium has long been a target for medicinal intervention due to the involvement of blood-brain barrier (BBB) inflammation in neurological disorders.[1] The healthy BBB is a metabolic and physical structure of the Central Nervous System (CNS) that creates a barrier between the body and neural tissue impermeable to most native and foreign substances whilst allowing the entry of oxygen and essential nutrients.[2, 3] The BBB *in vivo* controls permeability through the expression of

tight junctions, efflux pumps, receptors and the support of glial cells (astrocytes, pericytes, microglia). This extremely effective neuroprotective function also restricts entry of beneficial pharmacological agents necessary to treat neurological disorders.[4, 5] However, nanoparticles (NPs) have become a subject of intense investigation for the treatment of neurological disorders, as they are capable of interacting with the cellular transport machinery due to their small size, and are highly pharmacologically modifiable due to the large diameter to surface area ratio.[6-10] Additionally, the use of NPs as contrast agents for diagnosis is increasing, many of which would not be intended to reach the brain. Understanding the effect of NP exposure to biological entities under the criteria of cellular transportation and long-term toxicity is therefore of paramount importance.[11-16]

There has been an explosion in the number of studies of NP transport to the brain, most of which focussed on the potential of nanomaterials to cross biological barriers and/or biodistribute to the brain, and on the impacts of nanomaterials on the delicate tissues and cells of the CNS once across.[17-21] However, two as yet neglected areas of research are the investigation of the potential impact of NPs on the cells of the barrier themselves as a result of NP accumulation in the barrier, and the potential for signalling or other impacts to the brain without actual crossing of the NPs into the CNS (so-called indirect effects). Such indirect NP-induced signalling effects have been shown to occur across the placental barrier, with the barrier thickness affecting the signalling potential.[22, 23] Since the BBB is a single endothelial cell layer (supported by astrocytic end feet), it may be particularly vulnerable to overload as a result of accumulation of NPs. Uptake studies of a host of different NPs have shown that the final destination of the NPs is usually the lysosomes, for many different cell lines.[24, 25] Our own work has suggested that once in the lysosomes, there are no export pathways for NPs.[26, 27] However, this question has not yet been addressed for cellular barriers, where the focus has tended, as indicated above, to be on those NPs that cross the barrier, rather than on those NPs that accumulate within it.

The *in vitro* hCMEC/D3 BBB model is the closest human correlate to the human *in vivo* BBB available to evaluate NP interaction with a cellular barrier.[3] This can be further supported by direct/indirect co-culture with human astrocytes[28] to account for cell-cell signalling and other physiological effects that are missed in simple cell culture models. While there are well known limitations to barrier models for predicting *in vivo* effects, the advantage of barrier models lies in their ability to probe mechanistic issues. We have previously demonstrated that this model can be used to study NP interactions with, uptake into and transport across the BBB.[29] Our findings then, and on the basis of significant additional imaging work, suggested that only very small numbers of NPs cross the *in vitro* BBB. Building on that, the present paper investigates the effect of NP accumulation in the BBB on lysosome health and paracrine signalling, as it is clear that impacts on the BBB cells could have dramatic consequences for the vulnerable tissues protected by biological barriers.

Carboxylated polystyrene NPs (PS COOH NPs) are largely considered to be non-toxic.[7, 30] In this study we used fluorescently-labelled and unlabelled variants of PS COOH NPs as they are excellent model NPs widely used in the study of bionanointeractions,[30] due to their low toxicity and ease of visualisation. Additionally, the fact that they do not biodegrade over timescales relevant for uptake and impact studies means that it is possible to assess impacts directly related to the presence of the NPs themselves, without any complications from potential degradation products, or as a result of NP dissolution. While polystyrene is difficult to visualise using electron microscopy (given that its electron density is similar to that of the cellular background), the 100 nm PS COOH NPs are nevertheless easily discernible (as will transpire below) and as such were selected despite having been shown to enter cells less than smaller (e.g. 40 nm) variants.[31, 32] Therefore, in this initial study the *in vitro* hCMEC/D3 monolayer was exposed to 100 nm PS COOH NPs to test BBB endothelium uptake, lysosomal accumulation and paracrine signalling *in vitro*. Essentially, paracrine signalling in this case describes how NP exposure to the *in vitro* BBB monolayer can affect secreted signalling between endothelium and nearby glia without physical contact between the two cell types. TEM imaging of the *in vitro* BBB monolayer showed the accumulation of large amounts of PS COOH NPs

within the BBB lysosomes which did not degrade or clear in the short term. PS COOH NPs had no obvious toxic effect on the *in vitro* BBB using common toxicological testing methods (e.g. the MTS assay). However, a more sensitive cytokine array approach gave additional information on the impact of the accumulation of PS COOH NPs on the BBB monolayer. We looked at the possibility of NP exposure affecting the paracrine signalling from the endothelial layer to underlying glia. In the short term we found a low level of pro-inflammatory cytokine release from the BBB endothelium alone, which was significantly improved in the presence of glial cells growing beneath the monolayer, but not in direct contact with it. Thus, paracrine signalling does occur between *in vitro* BBB cells upon NP exposure, even with NPs which are generally considered to be essentially non-toxic. This suggests that such effects should be studied further, particularly in the case of 'known' toxic NPs.

Experimental

Cell culture

1 x 10^6 immortalized human brain capillary endothelial cells (hCMEC/D3) were seeded in a collagen coated flask (25 cm^2, Becton Dickinson) and supplemented with EBM-2 medium containing vascular endothelial growth factor (VEGF), insulin-like growth factor-1 (IL-1), epidermal growth factor (EGF), basic fibroblast growth factor (bFGF), fetal calf serum (2%), gentamicin sulphate/amphotericin B and hydrocortisone (Lonza Biosciences).

The hCMEC/D3 monolayer was prepared on a collagen coated 12-well plate for LysoTracker and uptake studies. 12-well plates were coated with 1 ml collagen (0.1 mg/ml rat tail collagen type 1, Sigma) on day of seeding and incubated at 37°C in a sterile incubator over 30 min. Each well was washed 3 times in PBS and allowed to dry for 30 min. hCMEC/D3 cells were seeded in 1 ml EBM-2 media (Lonza) at a density of $5{\cdot}10^4$ cells/well. Medium was replaced 6 h post seeding and then only once during the 7 days of barrier formation. For monolayer formation, cells were supplemented with growth factor depleted EBM-2 assay medium containing bFGF, 2% FCS, gentamicin sulphate/amphotericin B, hydrocortisone and 10 mM HEPES. Cells were cultured in an incubator at 37°C with 5% CO_2/95% air and saturated humidity. Cell culture medium was changed once weekly under monolayer formation conditions.

The *in vitro* BBB monolayer was grown on transwell filters for TEM experimentation (PET membrane, 1.12 cm^2, 0.4 µm pore size, Corning). Membrane inserts were coated with 200 µl collagen/fibronectin (15% rat tail collagen and 15% bovine fibronectin, Invitrogen) 1 day prior to use and stored at 37°C in a dry incubator. For TEM imaging, hCMEC/D3 cells were seeded in 500 µl assay media at a density of $5{\cdot}10^4$ cells per 1.2 cm^2 filter in the apical compartment and 1500 µl assay media in the basolateral compartment. Assay medium was changed 6 h post seeding and once weekly thereafter. Monolayers were used 7-10 days post-transwell seeding.

In the case of paracrine signalling experiments, a system composed of hCMEC/D3 cells and Normal Human primary Astrocytes (NHA) was set-up (hCMEC/D3-NHA-BBB). hCMEC/D3 cells were seeded on transwell inserts (PTFE membrane, collagen-coated, 3 µm pore size, Corning) as above. Normal human primary astrocytes (NHA) were grown in a 12 well plate in ABM medium at a seeding density of 5,000 cells/cm^2 (Lonza). NHA were seeded on the 12 well plate surface directly below the transwell filter 24 h after hCEMC/D3 seeding, as shown in Scheme 1.

Flow cytometry

Flow cytometry analysis was conducted 7-10 days after seeding on a 12 well plate allowing formation of the BBB monolayer as described above. For uptake experiments, hCMEC/D3 monolayers were exposed to fluorescent 100 nm PS COOH NPs at 25 µg/ml and 100 µg/ml from 3-72 h. After the required exposure, plates were washed three times with PBS and cells were harvested

with 0.05% Trypsin-EDTA 1x, centrifuged for 3 min at 1500 rpm at 20°C, fixed for 20 min with 4% formalin at room temperature and re-suspended in 1 ml PBS for analysis with an Accuri C6 flow cytometer. The time between fixation and measurement was kept constant for each experiment. 100 nm PS COOH NP fluorescence intensity from the cells was determined using 488 nm excitation and measuring emission at 530 nm. A total of 15,000 events were recorded for each sample. The data are represented as the mean cell fluorescence intensity and standard deviation between the replicas (n=3). For lysosomal accumulation studies, hCMEC/D3 cells were grown on 12 well plates as described above and exposed to non-fluorescent 100 nm PS COOH NPs at various concentrations (100 µg/ml-300 µg/ml) over 48 h. Cell harvesting was carried out as described above and live cells were incubated with 50 nM LysoTracker Red (Invitrogen) for 20 min at 37°C. LysoTracker fluorescence acquisition was carried out using 2 filters (530/40 nm and 575/25 nm) immediately after cell preparation. All flow cytometry was carried out in the Flow Cytometry Core Facility of the Conway Institute for Biomolecular and Biomedical Research, University College Dublin.

Transmission Electron Microscopy (TEM)

7 day old hCMEC/D3 monolayers were exposed to 100 µg/ml 100 nm PS COOH NPs over 4 and 28 h at 37°C. Permeable PET transwell filters containing a confluent monolayer of endothelial cells were fixed with glutaraldehyde (2.5%, v/v) in Sorensen phosphate buffer for 1 h at room temperature, and post-fixed with osmium tetroxide (1%, w/v) in de-ionised water for 1 h. After dehydration in a graded series of 70%, 90% and 100% ethanol and embedding in epoxy resin, 80 nm sections were cut perpendicular to the monolayer with a Leica Microtome, contrasted with 2% uranyl acetate and lead citrate, and examined with an electron microscope (TECNAI).

Paracrine Signalling Experiment

A human cytokine antibody array including 32 human cytokine targets was used in this experiment (MA6160, Panomics). Briefly, basal cell culture medium from control and treated hCMEC/D3 monolayer alone and hCMEC/D3-NHA-BBB systems were incubated with individual cytokine array membranes for 2 h at room temperature. Biotin-labelled antibodies were then added to the array membrane for 1 h at room temperature. Horseradish peroxidase labelled streptavidin (Streptavidin-HRP) was used to detect the antibody-protein complexes on the array membrane. Chemiluminescence was then used to visualise the cytokine signal with X-Ray film (Fuji) and densitometry was carried out using ImageJ (http://rsb.info.nih.gov/ij/).

Nanoparticle dispersion and characterisation

100 nm PS COOH NPs were purchased from Invitrogen (F8803). The size of 100 nm PS COOH NPs dispersed in assay media was determined with a Malvern Zetasizer 3000HSa. The NPs were diluted in 1.5 ml assay medium to reach a 100 µg/ml concentration. The solution of PS COOH NPs was incubated at 37°C in an orbital shaker over 4 h and sampled each hour. The measurements were conducted at 37°C by transferring 500 µL of the stock solution to a square cuvette for DLS analysis. DLS measures dynamic fluctuations of light scattering intensity caused by the Brownian motion of the particles. This technique yields a hydrodynamic radius, or diameter, calculated via the Stokes-Einstein equation from the aforementioned measurements.

Results

This study tested human BBB (hCEMC/D3) cell viability upon exposure to 40 nm, 100 nm and 200 nm PS COOH NPs at a relatively low concentration of 25 µg/ml and a relatively high concentration of 100 µg/ml. We found neither a size nor a concentration dependent alteration in hCMEC/D3 cell viability upon exposure to PS COOH NPs over the life time of the *in vitro* monolayer (72 h), as shown in Figure 1. However, it is worth noting that the number of NPs presented to the cells varied by a factor of ~125 from the 40 nm case to the 200 nm, as the studies were performed at constant particle mass. Literature reports the lack of toxicity upon interaction with PS COOH NPs to various cell types

including HeLa tumoural epithelial cells, lung epithelial cells and astrocytoma cell lines.[30] This is in contrast to amine-modified PS NPs which have been shown to be toxic to *in vitro* CNS cell lines due to cell membrane rupture and caspase activation.[11]

The 100 nm PS COOH NPs were then used for uptake, localisation and paracrine signalling studies. NP characterisation (size and zeta potential, in Supp Fig 1 and 2 respectively) indicated that in cell culture medium supplemented with 2 % bovine serum, stable dispersions were obtained and that the average size increased, while (absolute) zeta potential decreased, as a consequence of protein adsorption, protein corona formation[33] and likely partial agglomeration.

Evaluation of 100 nm PS COOH NP uptake and localisation in the hCMEC/D3 cells showed a lower level of uptake in the barrier (i.e. when cells are grown for 7 days) compared to that observed in the single cells upon short-term NP exposure (Supp Fig 3). This is perhaps unsurprising since hCMEC/D3 barrier formation involves the formation of tight junctions allowing the BBB monolayer to communicate fully and prohibit the entry of foreign material, a protective function for which the BBB is well known.[3] The 100 nm PS COOH NPs were internalised by the barrier and accumulated into lysosomes, as shown by TEM imaging (Figure 2).

At increasing exposure times, a plateau-like kinetics of 100 nm PS COOH NP uptake occurred in the hCMEC/D3 BBB monolayer from 24 h-72 h exposure (Supp Fig 3). It should also be noted that the non-confluent BBB cells also reached a plateau of uptake 24 h post NP exposure. Our previous work has shown similar plateau-like NP uptake kinetics in other cell lines, which has been attributed to dilution of NP load upon cell division,[27] an effect that is most likely not the (main) source of the plateau for the BBB monolayer. TEM imaging of the *in vitro* BBB showed an increase in lysosomal accumulation of 100 nm PS COOH NPs at increasing exposure times. Prolonged barrier exposure (28 h) to 100 nm PS COOH NP in fact showed that most lysosomes were filled with high numbers of NPs (Supp Fig 4). The size and spherical nature of the PS COOH NPs remained intact suggesting that the digestive enzymes of the lysosome had not (at least on this time scale) affected the structural integrity of the particles.

We then investigated the possible limitations of this model regarding the capacity of the BBB lysosomes for NP accumulation. By increasing the concentration of 100 nm PS COOH NPs presented to the BBB by two and three-fold, we tested whether the lysosomes would increase in size or possibly lose membrane integrity due to NP accumulation. Using acidotropic probes, such as LysoTracker, an eventual increase in lysosomal staining would be indicative of lysosomal swelling, while formation of a second peak at lower intensity could be sign of compromised lysosomal membrane integrity.[34] However, we found that increasing the concentration of 100 nm PS COOH NPs to 300 µg/ml over 48 h exposure did not greatly alter the lysosomal acidic compartments of the hCMEC/D3 monolayer, as shown in Figure 3. This may be explained by the relatively low uptake levels in the barrier, in comparison to single cells, or may suggest that the hCMEC/D3 barrier has a very high capacity to accommodate PS COOH NPs, and even at very high NP loading the lysosome size and integrity was not perturbed greatly. Time-dependent studies yield a similar conclusion (Supp Fig 5).

We then investigated whether accumulation of foreign material in barrier lysosomes triggered downstream inflammatory signalling mechanisms. Correct lysosome function is vital to cell health as lysosomal accumulation can lead to abnormal protein ubiquitination and downstream inflammatory signalling.[35] As barrier models are a useful approach to look at paracrine signalling from the endothelial cells lining the brain capillaries, we evaluated how capable an endothelial barrier is at dealing with a large accumulation of seemingly innocuous NPs over time. We found that conclusions regarding cytotoxicity, or lack thereof, may be somewhat misleading, as short term exposure of an *in vitro* BBB showed 100 nm PS COOH NPs to have a negative effect, albeit to a small degree, on the paracrine signalling from brain endothelium alone. A cytokine array containing 32 protein recognition sites highlighted VEGF and IL-4 signals as being released from the BBB monolayer into

the underlying cell culture medium 4 h post PS COOH NP exposure. However, the change in VEGF or IL-4 cytokine signalling was not significant compared to the untreated BBB monolayer (Figure 4A). Low level cytokine release, in the form of pro-inflammatory cytokine RANTES, was found upon 24 h exposure of the *in vitro* BBB to 100 nm PS COOH NPs compared to control (Figure 4B). However, RANTES is usually associated with an up-regulation in other inflammatory proteins such as IL-2 and IFN-y during inflammation, and such an up-regulation was not observed in the treated BBB samples. In addition, no regulation of the cell adhesion molecules tested (ICAM, VCAM) was found, as would be expected in normal type II activation of endothelial inflammation.

We finally exposed the BBB hCMEC/D3 monolayer to the same NPs in the presence of supporting normal human primary astrocytes (NHA). Growth of human astrocytes below the BBB endothelium monolayer allows the communication of supporting signals *in vitro*, which aids in mimicking a more realistic *in vivo* situation,[36] allowing these signalling pathways to occur. Prolonged exposure of the BBB monolayer to 100 nm PS COOH NPs led to an increase in secreted anti-inflammatory signals between the endothelial monolayer and the astrocytic cell layer grown in the chamber below it (Figure 5). The cytokine protein levels in this system were assayed using the cell culture medium from the lower compartment (see Scheme 1) i.e. from below the BBB endothelium monolayer (grown on the transwell filter membrane) and above the human astrocytes grown on the surface of the 12 well plate. In contrast to the secreted cytokine signal from the 100 nm PS COOH NP treated endothelial monolayer alone (Figure 4B), a down-regulation of RANTES signalling was found upon 100 nm PS COOH NP exposure to the endothelia-astrocyte BBB system (hCMEC/D3-NHA BBB). Down-regulation of tumour necrosis factor receptor 1 (TNFR1) secretion was also observed. A possible interpretation of the TNFR1 down-regulation is that it may be involved in impeding a persistent inflammatory signal between BBB endothelium and underlying astrocytes. We did not see a decrease in TNF itself, which is not surprising as there would be no need to down-regulate a protein if its mode of signalling has already been decreased. A significant up-regulation in Epidermal Growth Factor (EGF) signalling in the hCMEC/D3-NHA BBB system upon prolonged exposure to 100 nm PS COOH NPs may promote cell survival when endothelial BBB lysosomes are close to capacity in terms of their packing with NPs. These results indicate that when the astrocytes are added, some signalling molecules secreted by the endothelium in response to the presence of the PS COOH NPs are subsequently amplified by the astrocytes, whereas others are down-regulated. This suggests that accumulation of PS COOH NPs in lysosomes of the *in vitro* BBB endothelium monolayer in the presence of supporting astrocytic secretions could impede the signals that would lead to an inflammatory reaction and possible cell death.

Discussion

The *in vitro* BBB does not restrict the uptake of NPs completely; however, 100 nm PS COOH NP uptake is slowed down considerably in the BBB monolayer compared to that observed in single hCMEC/D3 cells. The exact cellular uptake mechanisms of unmodified engineered NPs are as yet unknown.[24, 30] However, they do seem to use energy dependent uptake routes that lead to accumulation in the lysosomes (i.e. the endo-lysosomal pathway). There is likely less exposed cell surface area upon hCMEC/D3 barrier formation compared to the single hCMEC/D3 cells. Therefore, there are less possible points of entry for NPs, whether they be specific or not, which could also contribute to the decreased 100 nm PS COOH NP uptake in the hCMEC/D3 barrier compared to the non-confluent cell format. Additional work is required to resolve this question.

TEM imaging of 100 nm PS COOH NPs that entered the hCMEC/D3 BBB monolayer showed the NPs largely accumulating in lysosomal compartments. These NPs were not seen to clear from the lysosomes over time (at least over the time scale investigated), nor were they degraded by this highly acidic compartment as the distinctly spherical structure was not altered over the time-course of our experiments (48 h), in agreement with previous observations for other NPs accumulating in the lysosomes.[24] This is in contrast to other studies that have suggested iron oxide NPs and carbon

nanotubes breakdown under biological conditions, albeit over longer timeframes. However, polystyrene has been shown to be resistant to thermal oxidation below 200°C, which is far above the viability limit of *in vitro* biological conditions.[37-39]

A high level of lysosomal accumulation was associated with a low level of cytokine signalling 24 h post exposure of the BBB monolayer to 100 nm PS COOH NPs. Inflammasome activation due to lysosome signalling is associated with an increase in activated IL1-beta levels, which were not found in this study.[40] The paracrine signalling between BBB endothelium and the underlying astrocytes upon 24 h exposure of the endothelium to 100 nm PS COOH NPs showed a decrease in pro-inflammatory cytokine signalling compared to control cultures not exposed to NPs. Müller et al. suggested a nanotoxicological classification system considering both particle size and biodegradability as important factors for nanotoxicity.[41] Thus, loading of the lysosomes with the non-degrading PS-COOH NPs appears to lead to some stress for the cells and to the observed increase in signalling.

To date, the literature mainly describes inflammation of the *in vitro* BBB upon exposure to known cytokines (TNFalpha, Il-4) eliciting a response thereafter.[42] Also, other *in vitro* barriers (placental and corneal), have shown a very low level of cytokine release upon NP exposure (CoCr NPs in this case),[22] suggesting that NPs can induce indirect (or paracrine) signalling effects on cells that have not been directly exposed to the NPs, and that these biological barriers may themselves be affected by NP accumulation.

Conclusions

TEM imaging showed accumulation, but not degradation, of 100 nm PS COOH NPs within the lysosomes of the *in vitro* BBB cells over time. Cytokine secretion analysis from the *in vitro* BBB post 24 h 100 µg/ml 100 nm PS COOH NP exposure showed a low level of pro-inflammatory RANTES protein secretion compared to control. In contrast, 24 h exposure of the *in vitro* BBB endothelium to 100 µg/ml 100 nm PS COOH NPs in the presence of underlying astrocytes caused a significant increase in pro-survival signalling.

The accumulation of NPs in the blood brain barrier demonstrated in this work, and the consequent slight increase in cytokine expression in the co-culture model compared to the endothelial cells alone, suggest that the endothelium itself might be a target for NPs. Therefore, there is a significant need to understand the consequences for barrier health, and signalling to cells on either side, as a result of NP accumulation in the barrier. The fact that the particles studied here were non-toxic and did not change the barrier function *per se* is especially important, as this would likely be the case for drug delivery vehicles or diagnostic NPs applied *in vivo*. Clearly more dramatic effects would likely result from accumulation of NPs that were themselves cytotoxic, such as induction of apoptosis of the barrier cells. However, from a toxicity viewpoint, it is the subtle effects, persisting over longer periods due to inability to clear or degrade NPs that are the true cause of concern in terms of the application of nanotechnologies, as is suggested by this body of work.

Overall, caution is required in future studies of long-term NP interaction and accumulation within cellular barriers, as general toxicity assays may be disguising significant signalling regulation during long-term accumulation. Bioaccumulation is clearly potentially relevant also to other cellular barriers (in addition to the BBB studied here, such as the foetal or gut barriers) and the indirect signalling effects demonstrated here may also be present in these cases. The methodologies employed here are thus well-placed to address such issues for other barriers.

In future, the scientific community needs more effective long term *in vitro* methods to study these signalling issues further, and significant effort should be invested to validate the relevance of such models for prediction of *in vivo* consequences.

Acknowledgements

This research has been supported by the EU FP7 Small Collaborative project NeuroNano, NMP4-SL-2008-214547 (M.N.R., M.B., I.L.), and by a UCD SEED grant (SF224). Part of this work was conducted under the framework of the INSPIRE programme, funded by the Irish Government's Programme for Research in Third Level Institutions, Cycle 4, National Development Plan 2007-2013 (D.Y., A.S.), as well as Science Foundation Ireland under Grant No. [09/RFP/MTR2425] (C.Å.) and EU FP7 via the small collaborative project NanoTransKinetics (grant no. NMP4-2010-EU-US-266737) (C.Å.). Use of the UCD Conway Imaging Facility and the UCD Electron Microscopy Core facility is also acknowledged.

Notes and References

Electronic Supplementary Information (ESI) available: nanoparticle characterisation, additional data on nanoparticle uptake and impact on lysosomes. See DOI: 10.1039/c3an01621h

1. B. V. Zlokovic, *Nature Rev Neurosci*, 2011, **12**, 723-738.
2. N. J. Abbott, L. Ronnback and E. Hansson, *Nature Rev Neurosci*, 2006, **7**, 41-53.
3. B. B. Weksler, E. A. Subileau, N. Perriere, P. Charneau, K. Holloway, M. Leveque, H. Tricoire-Leignel, A. Nicotra, S. Bourdoulous, P. Turowski, D. K. Male, F. Roux, J. Greenwood, I. A. Romero and P. O. Couraud, *FASEB J*, 2005, **19**, 1872-1874.
4. D. J. Begley, *Pharmacol. Ther.*, 2004, **104**, 29-45.
5. W. M. Pardridge, *Drug Discov. Today*, 2007, **12**, 54-61.
6. A. des Rieux, V. Fievez, M. Garinot, Y. J. Schneider and V. Preat, *J Control Release*, 2006, **116**, 1-27.
7. S. A. Galindo-Rodriguez, E. Allemann, H. Fessi and E. Doelker, *Crit Rev Ther Drug Carrier Syst*, 2005, **22**, 419-464.
8. A. Zensi, D. Begley, C. Pontikis, C. Legros, L. Mihoreanu, S. Wagner, C. Buchel, H. von Briesen and J. Kreuter, *J Control Release*, 2009, **137**, 78-86.
9. J. Kreuter, D. Shamenkov, V. Petrov, P. Ramge, K. Cychutek, C. Koch-Brandt and R. Alyautdin, *J Drug Target*, 2002, **10**, 317-325.
10. J. Kreuter, *Adv Drug Del Rev*, 2012, **64, Supplement**, 213-222.
11. M. G. Bexiga, J. A. Varela, F. Wang, F. Fenaroli, A. Salvati, I. Lynch, J. C. Simpson and K. A. Dawson, *Nanotoxicology*, 2010, **5**, 557-567.
12. A. Nel, T. Xia, L. Madler and N. Li, *Science*, 2006, **311**, 622-627.
13. G. Oberdorster, A. Elder and A. Rinderknecht, *J. Nanosci. Nanotechnol.*, 2009, **9**, 4996-5007.
14. G. Oberdorster, Z. Sharp, V. Atudorei, A. Elder, R. Gelein, W. Kreyling and C. Cox, *Inhal. Tox.*, 2004, **16**, 437-445.
15. S. T. Stern and S. E. McNeil, *Toxicol Sci*, 2008, **101**, 4-21.
16. K. Donaldson, V. Stone, C. Tran, W. Kreyling and P. Borm, *Occup Environ Med*, 2004, **61**, 727-728.
17. L. Zhang, R. Bai, B. Li, C. Ge, J. Du, Y. Liu, L. Le Guyader, Y. Zhao, Y. Wu, S. He, Y. Ma and C. Chen, *Toxicol Lett*, 2011, **207**, 73-81.
18. P. Kundu, C. Mohanty and S. K. Sahoo, *Acta Biomater*, 2012.

19. M. Yemisci, Y. Gursoy-Ozdemir, S. Caban, E. Bodur, Y. Capan and T. Dalkara, *Methods Enzymol*, 2012, **508**, 253-269.

20. C. Schleh, M. Semmler-Behnke, J. Lipka, A. Wenk, S. Hirn, M. Schaffler, G. Schmid, U. Simon and W. G. Kreyling, *Nanotoxicology*, 2012, **6**, 36-46.

21. A. Haase, S. Rott, A. Mantion, P. Graf, J. Plendl, A. F. Thunemann, W. P. Meier, A. Taubert, A. Luch and G. Reiser, *Toxicol Sci*, 2012, **126**, 457-468.

22. A. Sood, S. Salih, D. Roh, L. Lacharme-Lora, M. Parry, B. Hardiman, R. Keehan, R. Grummer, E. Winterhager, P. J. Gokhale, P. W. Andrews, C. Abbott, K. Forbes, M. Westwood, J. D. Aplin, E. Ingham, I. Papageorgiou, M. Berry, J. Liu, A. D. Dick, R. J. Garland, N. Williams, R. Singh, A. K. Simon, M. Lewis, J. Ham, L. Roger, D. M. Baird, L. A. Crompton, M. A. Caldwell, H. Swalwell, M. Birch-Machin, G. Lopez-Castejon, A. Randall, H. Lin, M. S. Suleiman, W. H. Evans, R. Newson and C. P. Case, *Nature Nanotechnol*, 2011, **6**, 824-833.

23. G. Bhabra, A. Sood, B. Fisher, L. Cartwright, M. Saunders, W. H. Evans, A. Surprenant, G. Lopez-Castejon, S. Mann, S. A. Davis, L. A. Hails, E. Ingham, P. Verkade, J. Lane, K. Heesom, R. Newson and C. P. Case, *Nature Nanotechnol*, 2009, **4**, 876-883.

24. K. Shapero, F. Fenaroli, I. Lynch, D. C. Cottell, A. Salvati and K. A. Dawson, *Mol Biosyst*, 2010, **7**, 371-378.

25. M. Al-Rawi, S. Diabate and C. Weiss, *Arch Toxicol*, 2011, **85**, 813-826.

26. A. Salvati, C. Åberg, T. dos Santos, J. Varela, P. Pinto, I. Lynch and K. A. Dawson, *Nanomedicine NBM*, 2011, **7**, 818-826.

27. J. A. Kim, C. Åberg, A. Salvati and K. A. Dawson, *Nature Nanotechnol*, 2012, **7**, 62-68.

28. K. Hatherell, P. O. Couraud, I. A. Romero, B. Weksler and G. J. Pilkington, *J Neurosci Methods*, 2011, **199**, 223-229.

29. M. Nic Raghnaill, M. Brown, D. Ye, M. Bramini, S. Callanan, I. Lynch and K. A. Dawson, *Eur J Pharm Biopharm*, 2011, **77**, 360-367.

30. T. dos Santos, J. Varela, I. Lynch, A. Salvati and K. A. Dawson, *PLoS One*, 2011, **6**, e24438.

31. B. D. Chithrani, A. A. Ghazani and W. C. W. Chan, *Nano letters*, 2006, **6**, 662-668.

32. J. A. Varela, M. G. Bexiga, C. Åberg, J. C. Simpson and K. A. Dawson, *Journal of nanobiotechnology*, 2012, **10**, 39.

33. M. P. Monopoli, C. Åberg, A. Salvati and K. A. Dawson, *Nature Nanotechnol*, 2012, **7**, 779-786.

34. F. Wang, Y. Lu, M. P. Monopoli, P. Sandin, E. Mahon, A. Salvati and K. A. Dawson, *Nanomedicine NBM*, 2013, In Press.

35. A. Tessitore, M. Pirozzi and A. Auricchio, *Pathogenetics*, 2009, **2**, 4.

36. N. J. Abbott, A. A. Patabendige, D. E. Dolman, S. R. Yusof and D. J. Begley, *Neurobiol Dis*, 2009, **37**, 13-25.

37. M. Marek and L. Viererbl, *Appl Radiat Isot*, 2004, **61**, 1051-1055.

38. V. E. Kagan, N. V. Konduru, W. Feng, B. L. Allen, J. Conroy, Y. Volkov, Vlasova, II, N. A. Belikova, N. Yanamala, A. Kapralov, Y. Y. Tyurina, J. Shi, E. R. Kisin, A. R. Murray, J. Franks, D. Stolz, P. Gou, J. Klein-Seetharaman, B. Fadeel, A. Star and A. A. Shvedova, *Nature Nanotechnol*, 2010, **5**, 354-359.

39. M. Levy, F. Lagarde, V. A. Maraloiu, M. G. Blanchin, F. Gendron, C. Wilhelm and F. Gazeau, *Nanotechnology*, 2010, **21**, 395103.

40. L. J. Mawhinney, J. P. de Vaccari Rivero, G. A. Dale, R. W. Keane and H. M. Bramlett, *BMC Neurosci*, 2011, **12**, 123.

41. R. H. Muller, S. Gohla and C. M. Keck, *Eur J Pharm Biopharm*, 2011, **78**, 1-9.

42. E. Fasler-Kan, C. Suenderhauf, N. Barteneva, B. Poller, D. Gygax and J. Huwyler, *Brain Res*, 2010, **1354**, 15-22.

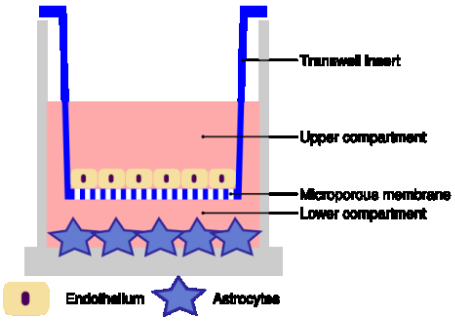

Scheme 1 Transwell hCMEC/D3-NHA-BBB system including hCMEC/D3 ('endothelium') and NHA ('astrocytes') in co-culture.

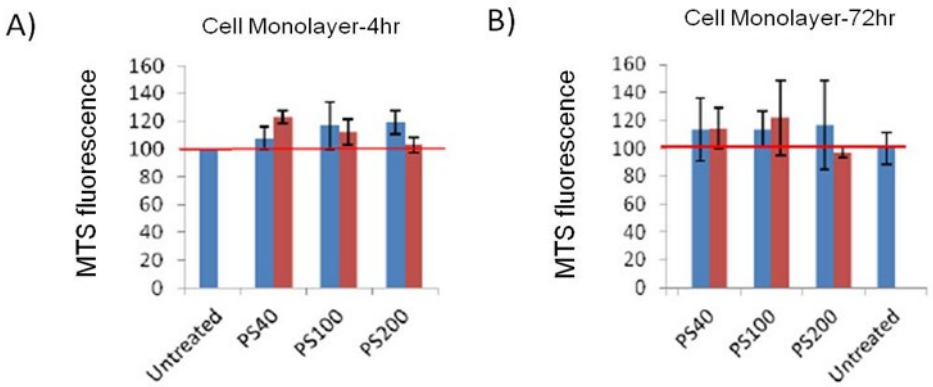

Fig. 1 PS COOH NPs have no significant effect on *in vitro* BBB cell viability over time. The 7 day old hCMEC/D3 barrier was exposed to two concentrations (Blue: 25 µg/ml; Red: 100 µg/ml) of 40 nm, 100 nm and 200 nm PS COOH NPs (PS40, PS100, PS200, respectively) over 4 or 72 h and evaluated under the parameter of cell viability. All data was normalised to a time matched control (Untreated) (n=3). (A) An acute 4 h exposure of the *in vitro* BBB to 40 nm, 100 nm and 200 nm PS COOH NPs did not alter the cell viability of treated samples compared to control. (B) A prolonged 72 h exposure of the *in vitro* BBB to the PS COOH NPs did not cause a significant alteration in cell viability compared to control.

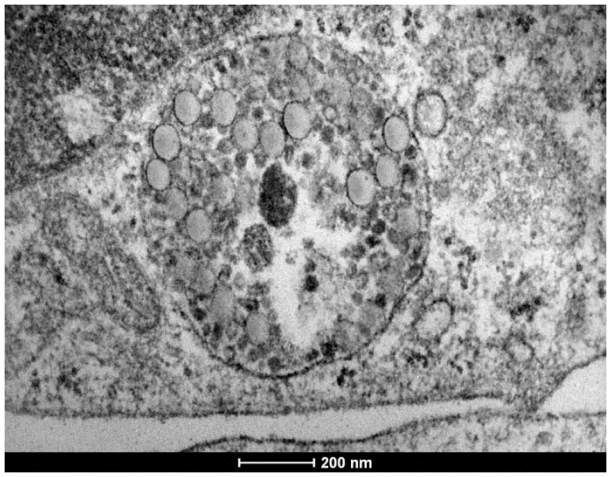

Fig. 2 TEM imaging of *in vitro* BBB 4 h post NP exposure showing lysosomal accumulation of 100 nm PS COOH NPs. Representative image of 100 nm PS COOH NP accumulation in BBB lysosomes 4 h post exposure (NP concentration 100 µg/ml).

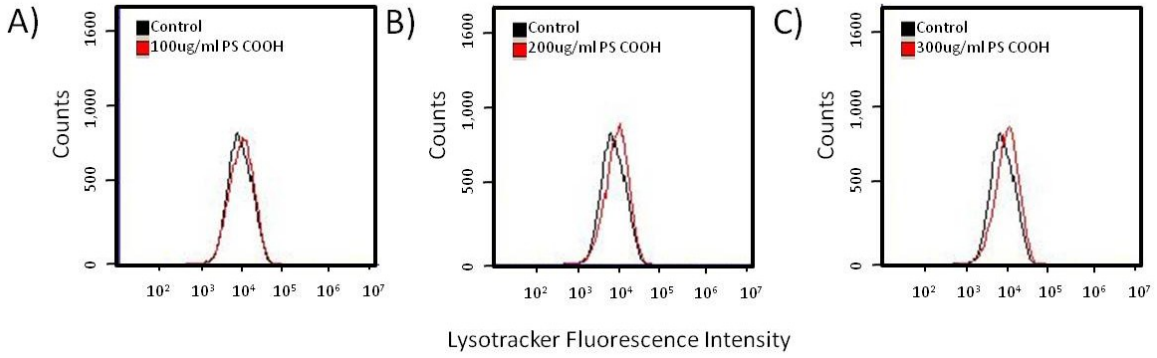

Fig. 3 Prolonged high dose exposure of hCMEC/D3 BBB endothelium monolayer to 100 nm PS COOH NPs does not alter the lysosomal compartments greatly. LysoTracker staining of hCMEC/D3 barrier cells post incubation with increasing concentrations of 100 nm PS COOH NPs showed no significant changes in the intensity of acidic lysosomal compartments over 48 h compared to control. Black: LysoTracker distribution in untreated control hCMEC/D3 barrier cells. Red: LysoTracker distribution in hCMEC/D3 barrier cells exposed to (A) 100 µg/ml, (B) 200 µg/ml and (C) 300 µg/ml of 100 nm PS COOH NPs.

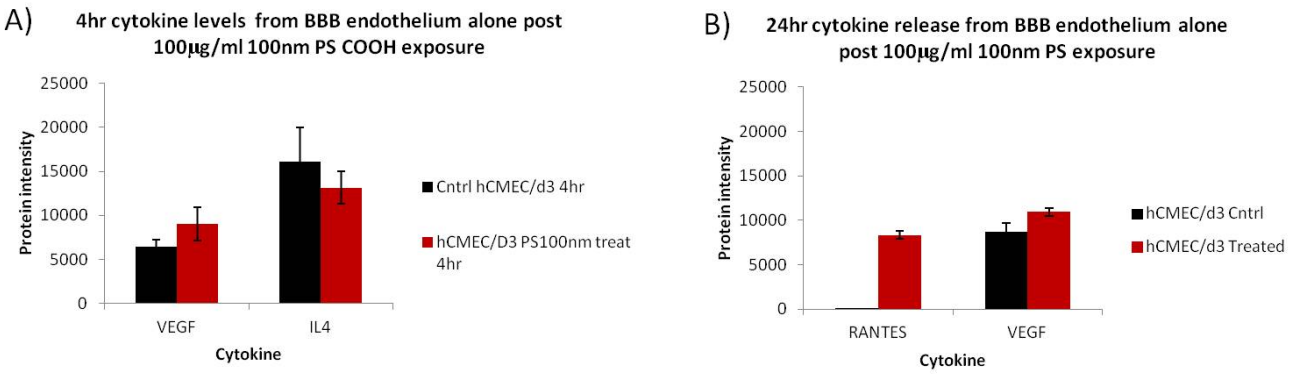

Fig.4 Cytokine signalling from the *in vitro* BBB post exposure to 100 nm PS COOH NPs. (A) 4 h exposure of *in vitro* BBB monolayer to 100 µg/ml 100 nm PS COOH NPs showed basal release of 2 cytokines (VEGF and IL-4). However, the difference in the level of VEGF or IL-4 in the treated cells (Treated) compared to control (Cntrl) after exposure for 4 h was not statistically significant. (B) In contrast, 24 h exposure of the BBB endothelium alone to PS COOH NPs showed a significant increase in RANTES expression in treated cells compared to control. Protein intensities are in arbitrary units.

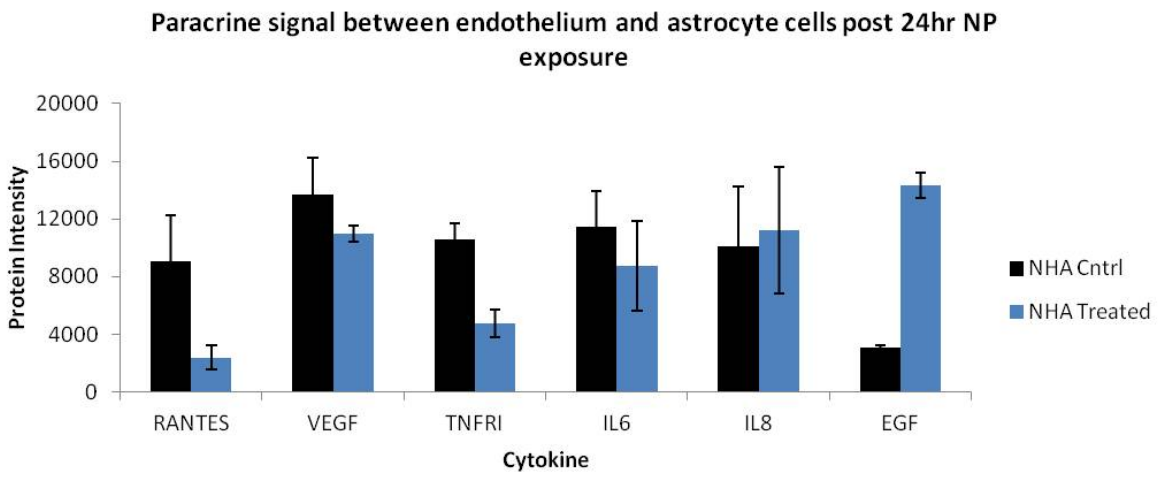

Fig. 5 Astrocyte communication with vascular endothelium stimulates cell survival signals within the *in vitro* BBB post exposure to 100 nm PS COOH NPs. A human cytokine array was used to investigate paracrine signalling between human endothelia and astrocytes post 100 µg/ml 100 nm PS COOH NP exposure (Blue bars) in comparison to untreated cells (Black bars). Regulation of 6 cytokines, out of a possible 32, was found between endothelium and astrocytes. The transwell system was used to grow a monolayer of endothelium on the filter support in a 12 well plate. Normal human primary astrocytes were grown on the bottom of the 12 well plate, directly underneath the filter supporting the endothelial layer (as shown in Scheme 1). 100 µg/ml 100 nm PS COOH NPs were exposed to the *in vitro* BBB endothelium monolayer for 24 h and the solution between the basal membrane of the endothelium and the astrocytic cells was investigated (i.e from the lower compartment in Scheme 1). Pro-inflammatory cytokines RANTES and TNFR1 showed a strong trend of down-regulation in the treated samples (Blue bars) compared to untreated controls (Black bars). Significant up-regulation of pro-survival protein EGF in NP treated model compared to control (Students two-tailed *t* Test, $p<0.01$) was also observed. Protein intensities are in arbitrary units.